Am J Physiol Lung Cell Mol Physiol 312: L334–L347, 2017.
First published December 23, 2016; doi:10.1152/ajplung.00059.2016.

RESEARCH ARTICLE

Targeted epigenetic editing of SPDEF reduces mucus production in lung epithelial cells

Juan Song,[1,2,3] David Cano-Rodriquez,[1] Melanie Winkle,[1] Rutger A. F. Gjaltema,[1] Désirée Goubert,[1] Tomasz P. Jurkowski,[4] Irene H. Heijink,[1,2] Marianne G. Rots,[1]* and Machteld N. Hylkema[1,2]*

[1]*University of Groningen, University Medical Center Groningen, Department of Pathology and Medical Biology, Groningen, The Netherlands;* [2]*University of Groningen, University Medical Center Groningen, Groningen Research Institute for Asthma and COPD, Groningen, The Netherlands;* [3]*Tianjin Medical University, School of Basic Medical Sciences, Department of Biochemistry and Molecular Biology, Department of Immunology, Tianjin, China; and* [4]*Institute of Biochemistry, Faculty of Chemistry, University of Stuttgart, Stuttgart, Germany*

Submitted 5 February 2016; accepted in final form 20 December 2016

Song J, Cano-Rodriguez D, Winkle M, Gjaltema RA, Goubert D, Jurkowski TP, Heijink IH, Rots MG, Hylkema MN. Targeted epigenetic editing of SPDEF reduces mucus production in lung epithelial cells. *Am J Physiol Lung Cell Mol Physiol* 312: L334–L347, 2017. First published December 23, 2016; doi:10.1152/ajplung.00059.2016.—Airway mucus hypersecretion contributes to the morbidity and mortality in patients with chronic inflammatory lung diseases. Reducing mucus production is crucial for improving patients' quality of life. The transcription factor SAM-pointed domain–containing Ets-like factor (*SPDEF*) plays a critical role in the regulation of mucus production and, therefore, represents a potential therapeutic target. This study aims to reduce lung epithelial mucus production by targeted silencing *SPDEF* using the novel strategy, epigenetic editing. Zinc fingers and CRISPR/dCas platforms were engineered to target repressors (KRAB, DNA methyltransferases, histone methyltransferases) to the *SPDEF* promoter. All constructs were able to effectively suppress both *SPDEF* mRNA and protein expression, which was accompanied by inhibition of downstream mucus-related genes [anterior gradient 2 (*AGR2*), mucin 5AC (*MUC5AC*)]. For the histone methyltransferase G9A, and not its mutant or other effectors, the obtained silencing was mitotically stable. These results indicate efficient *SPDEF* silencing and downregulation of mucus-related gene expression by epigenetic editing, in human lung epithelial cells. This opens avenues for epigenetic editing as a novel therapeutic strategy to induce long-lasting mucus inhibition.

SPDEF; epigenetic editing; mucus production; DNA methylation

AIRWAY EPITHELIAL MUCUS SECRETION and mucociliary clearance play a key role in protective innate immune responses against inhaled noxious particles and microorganisms. However, excessive mucus production and secretion contribute to the pathogenesis of several chronic inflammatory lung diseases, such as asthma and chronic obstructive pulmonary disease (COPD) (9, 11, 27). In patients with asthma and COPD, mucus hypersecretion is associated with cough and sputum production, respiratory infections, accelerated lung function decline, exacerbations, and mortality (23, 34). Therefore, targeted treatment of pathologic airway mucus secretion is expected not only to improve symptoms of cough and dyspnea, but also to decrease the frequency of disease-related exacerbations and decelerate disease progression. In the past few years, in preclinical models relevant to COPD, several drugs were shown to reduce mucus hypersecretion (21). However, none of these drugs target the mucus-producing cell itself.

Airway mucus contains mostly water and secreted mucins that contribute to the viscosity and elasticity of mucus gels. Mucin 5AC (*MUC5AC*) is the major secreted mucin, which is mainly produced by goblet cells in the airway epithelium. In chronic respiratory diseases, mucus hypersecretion is highly associated with increased numbers of goblet cells, as well as upregulated levels of mucin synthesis and secretion (9). SAM pointed domain-containing Ets transcription factor (*SPDEF*) has been reported to be a core transcription factor (TF) that, within a large network of genes, controls mucus production and secretion (6, 22, 35). In lung, *SPDEF* is selectively expressed in goblet cells lining the airways of patients with chronic lung disease (6) and mice exposed to allergens (25). In mice, the absence of *SPDEF* was shown to protect from goblet cell development after allergen exposure (6, 26). Moreover, knockdown of *SPDEF* with small interfering RNA (siRNA) was found to significantly reduce the expression of IL-13-induced *MUC5AC* expression and anterior gradient 2 (*AGR2*) expression, which encodes a potential chaperone required for mucin packaging, in the human bronchial epithelial cell line 16HBE (36). These observations suggest that *SPDEF* could be a potential therapeutic target for airway mucus hypersecretion. In this study, we set out to silence *SPDEF* expression by epigenetic editing. Epigenetic editing is a novel approach to modulate epigenetic states locally by targeting an epigenetic enzyme to the locus of interest via DNA-targeting systems, such as zinc fingers (ZFs), transcription activator-like effectors, or clustered regularly interspaced short palindromic repeats (CRISPRs) (5, 8, 17, 33). Compared with artificial transcription factors (ATFs), which exploit programmable DNA-binding platforms to target transcriptional activators or repressors with no catalytic domain (such as super KRAB domain, SKD), epigenetic editing has the promise to induce stable and inheritable gene modulation (4, 31). In this study, we provide proof-of-concept that *SPDEF*

* M. G. Rots and M. N. Hylkema contributed equally to this article.
Address for reprint requests and other correspondence: M. Hylkema, Dept. of Pathology and Medical Biology EA10, University Medical Center Groningen, Hanzeplein 1, 9713 GZ Groningen, The Netherlands (e-mail: m.n.hylkema@umcg.nl).

provides a promising target for epigenetic editing to prevent epithelial *MUC5AC* expression.

MATERIALS AND METHODS

Cell culture. Human bronchial epithelial 16HBE 14o- (16HBE) and BEAS-2B, mucoepidermoid carcinoma NCI-H292 and type II alveolar carcinoma A549 cell lines were cultured as previously described (15). The human embryonic kidney (HEK) 293T cell line [obtained from American Type Culture Collection (ATCC), Manassas, VA] and the breast cancer cell line MCF7 (obtained from ATCC: HTB-22) were cultured in DMEM (BioWhittaker, Verviers, Belgium). All culture media were supplemented with 2 mmol/l L-glutamine, 50 μg/ml gentamicin, and 10% FBS (BioWhittaker).

Plasmids constructs. Four 18-bp ZF protein target sites were selected within the *SPDEF* promoter using the website www.zincfingertools.org, as previously described (16). The target sequences are shown in Fig. 2*A*. The DNA sequences encoding the ZFs were synthesized by Bio Basic Canada. The fragments encoding the ZFs were digested with *Bam*HI/ *Nhe*I restriction enzymes (Thermo Fisher Scientific, Carlsbad, CA) and cloned into a SKD-NLS-ZF-TRI FLAG backbone, which encodes SKD, a triple-FLAG tag, and a nuclear localization signal (NLS) or a ZF-NLS-VP64-TRI FLAG backbone, which encodes a tetramer of Herpes Simplex Virus Viral Protein 16 (VP64). Then, the SKD-NLS-ZF SPDEF-TRI FLAG fragments and the ZF SPDEF- NLS-VP64-TRI FLAG were *Xba*I/ *Not*I (Thermo Fisher Scientific) digested and subcloned into a dual-promoter lentiviral vector pCDH-EF1-MCS-BGH PCK-GFP-T2A-Puro (SBI, cat. no. CD550A-1), obtaining constructs CD550A-1 SKD-ZF SPDEF and CD550A-1 ZF SPDEF-VP64. To obtain the constructs CD550A-1 ZF SPDEF-DNMT3A, the DNMT3A catalytic domain (kindly provided by Dr. A Jeltsch) was digested from pMX-ZF-DNMT3A-IRES-GFP with *Asc*I and *Pac*I, to replace VP64 in the CD550A-1 ZF SPDEF-VP64 vector. Catalytically mutant of DNMT3A (E74A) (13) was generated by PCR-mediated site-directed mutagenesis on CD550A-1 ZF SPDEF-DNMT3A. To obtain the constructs CD550A-1 ZF SPDEF-G9a and CD550A-1 ZF SPDEF-G9a W1050A, the G9a catalytic domain and its mutant were digested from pMX-E2C-G9a and pMX-E2C-G9a W1050A (10) with *Asc*I and *Pac*I, to replace VP64 in the CD550A-1 ZF SPDEF-VP64. To construct the CD550A-1 ZF SPDEF without effector domains (EDs) (SPDEF-NOED), VP64 in the CD550A-1 ZF SPDEF-VP64 was swapped out with PCR by a multiple cloning site, including restriction sites for *Asc*I, *Nsil*, *Bcl*I, *Swa*I, and *Pac*I. The primer information is presented in Table 1. pHAGE EF1α dCas9-VP64 lentiviral construct was a gift from Rene Maehr & Scot Wolfe (Addgene plasmid no. 50918) (18) and the single-chain guide RNA-encoding plasmid MLM3636 was a gift from Keith Joung (Addgene plasmid no. 43860). An additional multiple cloning site was added by replacing the VP64 activator with a sequence containing a *Mlu*I restriction site. To obtain the dCas9-epigenetic editor constructs, the G9a catalytic domain and its mutant, the SUV39h1 catalytic domain (10), and the catalytic domain of EZH2 (SET) and its mutant were digested out from pMX-ZF-IRES-GFP with *Mlu*I and *Not*I and subcloned into the empty pHAGE EF1α dCas9. The SKD domain and the DNMT3A3L catalytic domain and its catalytic mutant (29) were subcloned by amplifying with primers containing *Mlu*I and *Not*I overhangs. Cloning of guide RNAs (gRNA)

Table 1. *PCR and sequencing primers*

Primer Name	Sequence (5′–3′)	Application
SPDEF Pyro-A F	GGGTTATGGGAGAGTAAGTTGT	PCR and sequencing for SPDEF-A pyrosequencing
SPDEF Pyro-A R	[Biotin]TCTATACCCCACAAAATCCTCAT	
SPDEF Pyro-A Seq	GTTGTTGGTTGGTTT	
SPDEF Pyro-B/C F	GGATTTTGTGGGGTATAGAGAA	PCR and sequencing for SPDEF-B/C pyrosequencing
SPDEF Pyro-B/C R	[Biotin]ATTACTACATAACCACTCAACTCATATT	
SPDEF Pyro-B Seq	GGGGTATAGAGAATATAGTT	
SPDEF Pyro-C Seq	TTTAGAATTTTAGTTTTGGATTTA	
SPDEF Pyro-D/E F	ATGAGTTGAGTGGTTATGTAGTAAT	PCR and sequencing for SPDEF-D/E pyrosequencing
SPDEF Pyro-D/E R	[Biotin]CCAACCCAAAACTACCTACTAAC	
SPDEF Pyro-D Seq	AGTGGTTATGTAGTAATTAATG	
SPDEF Pyro-E Seq	AATTAGGTTTTGGTTAATTT	
DNMT3a-E74A F	CATTGCCTCCGCCGTGTGTGAGG	PCR for DNMT3a-E74A site mutagenesis
DNMT3a-E74A R	TAGCGGTCCACTTGGATGC	
NOED F	CGCGCCATGCATGATCATTTAAATTTAAT	PCR for NOED cloning
NOED R	TAAATTTAAATGATCATGCATGG	
SPDEF-ChIP-region 1 F	GCATGGGTGGTTCTGGATCT	ChIP-qRT-PCR for SPDEF region 1
SPDEF-ChIP-region 1 R	GCCAGAGATACGTCGAGTGG	
SPDEF-ChIP-region 2 F	GCAGCAACCAATGAACGAGTG	ChIP-qRT-PCR for SPDEF region 2
SPDEF-ChIP-region 2 R	ATTAACCCTTGCAGGTCTCCC	
SPDEF-ChIP-region 3 F	CCAGCACATTCCTGCACTCT	ChIP-qRT-PCR for SPDEF region 3
SPDEF-ChIP-region 3 R	CAACCTGAGGGGCTTGCAG	
FLAG-F	TGAATCGGTAGGAATTCGCGG	qRT-PCR for *FLAG*
FLAG-R	GGGAGGGGCAAACAACAGAT	
GAPDH-F	CCACATCGCTCAGACACCAT	qRT-PCR for *GAPDH*
GAPDH-R	GCGCCCAATACGACCAAAT	
ACTB-F	CCAACCGCGAGAAGATGA	qRT-PCR for *ACTB*
ACTB-R	CCAGAGGCGTACAGGGATAG	
RELA-F	CGGGATGGCTTCTATGAGG	qRT-PCR for *RELA*
RELA-R	CTCCAGGTCCCGCTTCTT	
TP53-F	GCTCAAGACTGGCGCTAAAA	qRT-PCR for *TP53*
TP53-R	GTCACCGTCGTGGAAAGC	
PLOD2-F	GGGAGTTCATTGCACCAGTT	qRT-PCR for *PLOD2*
PLOD2-R	GAGGACGAAGAGAACGC	
CDKN1A-F	TCACTGTCTTGTACCCTTGTGC	qRT-PCR for *CDKN1A*
CDKN1A-R	GGCGTTTGGAGTGGTAGAAA	

qRT-PCR, quantitative RT-PCR.

was achieved as previously described (4). Briefly, pairs of DNA oligonucleotides encoding 20-nucleotide gRNA targeting sequences were annealed together to create double-stranded DNA fragments with 4-bp overhangs. These fragments were ligated into *BsmB*I-digested plasmid pMLM3636. Two gRNAs were designed to bind close to the region where ZF3 and ZF4 bind (Fig. 2*A*) (GCATGGATCCCCCAGCAAGG and CCTCAGGTTGGGCCTTGCCA, respectively) and a third gRNA was designed to bind just before transcription start site (CTGGCCAACTCTTCATCTCG). We verified all constructs by DNA Sanger sequencing (Baseclear, Leiden, The Netherlands).

Lentiviral transduction. The lentiviral CD550A-1 constructs, encoding the *SPDEF*-targeting ATFs and epigenetic editors, were cotransfected with the third-generation packaging plasmids pMDLg/pRRE, pRSV-Rev, and pMSV-VSVG into HEK293T cells using the calcium phosphate transfection method to produce lentiviral particles. The supernatant of HEK293T cells containing virus was harvested at 48 and 72 h after transfection. Host A549 cells were seeded in six-well plates with a density of 80,000 cells per well and transduced on two consecutive days with the viral supernatant, supplemented with 8 μg/ml polybrene (Sigma-Aldrich, Zwijndrecht, The Netherlands). The positive transduced cells were selected in 8 μg/ml puromycin-supplemented medium for 4 days from 72 h after the last transduction and then were cultured in 1 μg/ml puromycin-supplemented medium. Medium was refreshed every 2–3 days. Ten days after the last transduction, cells were harvested for Western blot analysis, as well as RNA and DNA extraction. In the meantime, cells were grown on coverslips for immunocytochemistry and were harvested for chromatin immunoprecipitation.

Generation of MCF7 stable cell lines. The lentiviral pHAGE-EF1α constructs, encoding the dCas9-SKD and epigenetic editors, were cotransfected with the second-generation packaging plasmids psPAX2 and pMD2.G-VSV-G into HEK293T cells using Lipofectamine LTX-PLUS (Life Technologies) to produce lentiviral particles. The supernatant of HEK293T cells containing virus was harvested at 48 and 72 h after transfection. Host MCF7 cells were seeded in six-well plates with a density of 80,000 cells per well and transduced on two consecutive days with the viral supernatant, supplemented with 8 μg/ml polybrene (Sigma-Aldrich). The positive transduced cells were selected in 8 μg/ml puromycin-supplemented medium for 4 days from 72 h after the last transduction and then were cultured in 1 μg/ml puromycin-supplemented medium.

gRNA transfections. To transiently transfect the MLM3636 plasmids containing gRNA constructs, 500,000 of each stable MCF7 cells were seeded into six-well plates the day before transfection. For all experiments, a total of 2 μg of a combination of three gRNA plasmids were cotransfected using 2 μl PLUS reagent and 4 μl Lipofectamine LTX. The cells were then collected two days after transfection to isolate RNA and subcultured for additional 12 days.

Detection of mRNA expression by quantitative real-time PCR. Total RNA was extracted from A549 cells using TRIzol reagent (Thermo Fisher Scientific), and 500 ng was used for cDNA synthesis with random primers using Superscript II RNase H-RT (Thermo Fisher Scientific). *SPDEF*, *MUC5AC*, *AGR2*, and *GAPDH* expression was quantified using qPCR MasterMix Plus (Eurogentec, Seraing, Belgium) and TaqMan gene expression assays (*SPDEF*: Hs01026050_m1; *MUC5AC*: Hs00873651_Mh; *AGR2*: Hs00356521_m1; *GAPDH*: Hs02758991_g1; Thermo Fisher Scientific), mRNA expression of the fusion proteins (FLAG tag), procollagen-lysine,2-oxoglutarate 5-dioxygenase 2 (*PLOD2*), tumor protein P53 (*TP53*), RELA proto-oncogene, NF-κB subunit (*RELA*), cyclin-dependent kinase inhibitor 1A (*CDKN1A*), and β-actin (*ACTB*) using SYBR Green PCR Master Mix (Thermo Fisher Scientific) and gene-specific primers (Table 1) with the LightCycler 480 real-time PCR system (Roche, Basel,

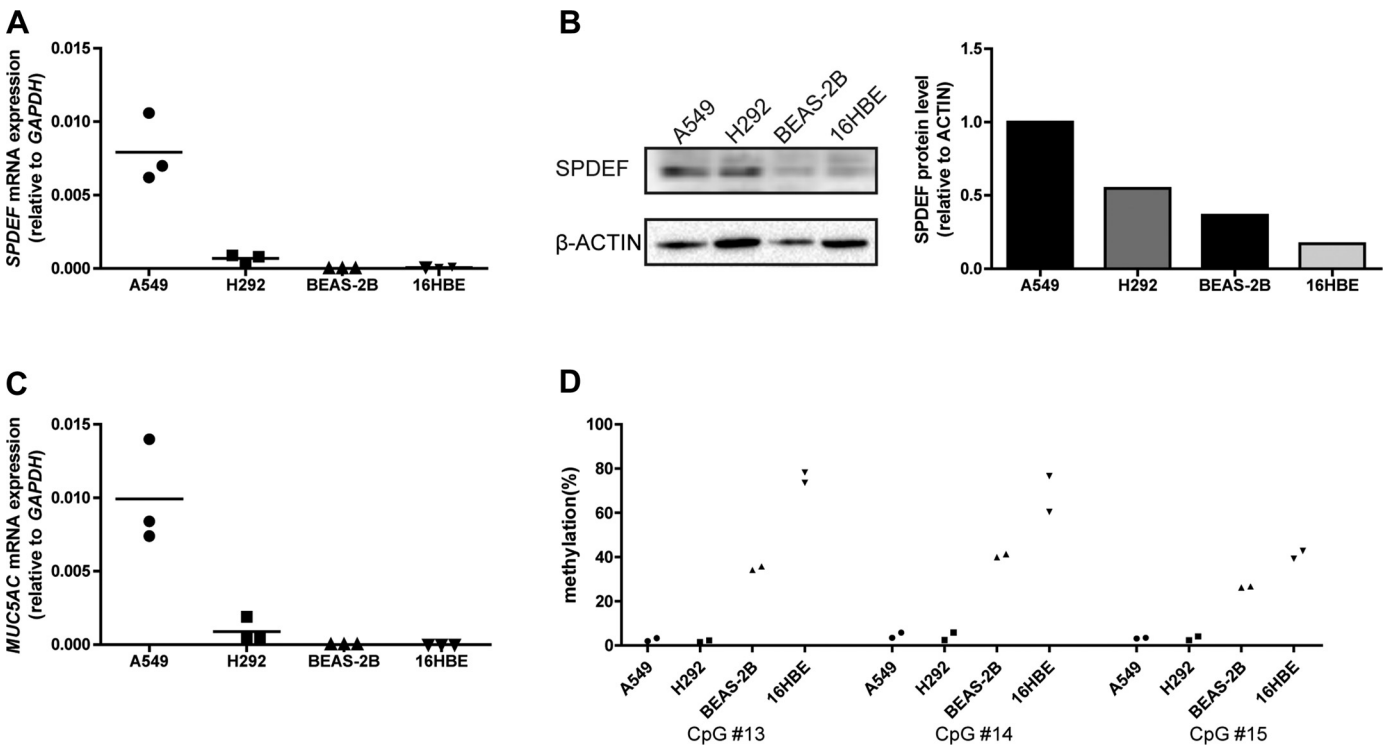

Fig. 1. Expression of SAM-pointed domain–containing Ets-like factor (*SPDEF*) (mRNA and protein) is associated with DNA methylation and *MUC5AC* expression. Quantification of the mRNA levels of *SPDEF* (*A*) and *MUC5AC* (*C*) in a panel of human epithelial cell lines (A549, H292, BEAS-2B, and 16HBE) by quantitative RT-PCR. Dot plots represent the mean and variation of three independent experiments. *B*: visualization of SPDEF protein expression (*left*) and quantification relative to β-actin (*right*), as conducted by Western blot analysis ($n = 1$). An anti-β-actin antibody was used as a loading control. *D*: quantitative analysis of the methylation levels of three CpG sites surrounding transcription start site (TSS) by pyrosequencing. Scatterplots show two independent experiments.

Switzerland). Data were analyzed with LightCycler 480 SW 1.5 software (Roche) and the Fit points method, according to the manufacturer's instructions. Expression levels relative to *GAPDH* were determined with the formula $2^{-\Delta Cp}$ (Cp denotes crossing points).

Methylation analysis by pyrosequencing. For DNA methylation analysis of the target regions, genomic DNA was extracted with chloroform-isopropanol and was bisulfite converted using the EZ DNA methylation kit (Zymo Research), following the manufacturer's protocol. Bisulfite-converted DNA was analyzed by pyrosequencing, as previously described (7). The primer information for pyrosequencing is presented in Table 1.

Histone modification analysis by chromatin immunoprecipitation and quantitative PCR. Histone modification induced by ZFs-G9a was analyzed by ChIP, as previously described (12). Briefly, A549 cells were fixed with 1% formaldehyde at 37°C for 10 min and subsequently lysed and sonicated using a Bioruptor (High, 30 s on, 30 s off; total time 15 min; Diagenode, Denville, NJ). Sheared chromatin was cleared by a centrifuge at 4°C (12,000 *g*, 10 min). Four micrograms of specific antibodies [normal rabbit IgG (abcam, ab46540), H3K9me2 (07–441; Millipore, Billerica, MA)] were bound to 50 μl of magnetic Dynabeads (Thermo Fisher Scientific) during 15-min incubation, then unbound antibodies were washed off. Sheared chromatin (0.25 million cells) was added to the antibody-precoated magnetic Dynabeads (rotating overnight at 4°C). Next day, the magnetic Dynabeads were washed three times with PBS, and chromatin was eluted with 1% (wt/vol) SDS and 100 mmol/l $NaHCO_3$. Subsequently, the elutions were treated with RNase (Roche) for 4 h and proteinase K (Roche) for 1 h at 62°C. Then, the column purified DNA (Qiagen, Hilden, Germany) could be analyzed with quantitative PCR (qPCR).

To assess the induction of histone marks and their spreading, several primer pairs were used for the SPDEF promoter (Table 1). qPCR was conducted using SYBR Green PCR Master Mix (Thermo

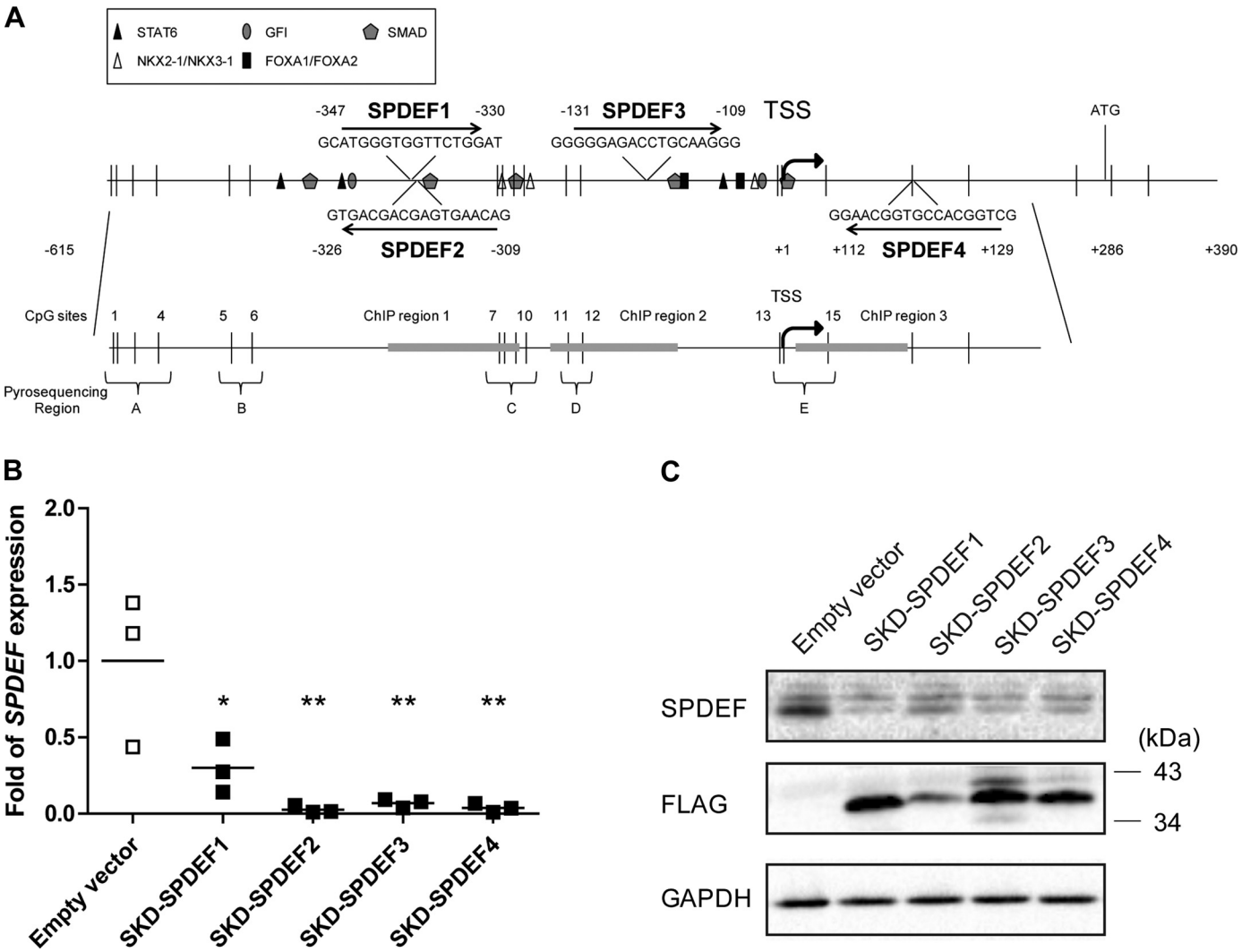

Fig. 2. *SPDEF*-targeted silencing by ATFs in A549 cells. *A*: schematic representations of the promoter region of the *SPDEF* gene, outlining the putative binding sites for transcription factors (STAT6, NKX2-1/NKX3-1, GFI, FOXA1/FOXA2, SMAD) (MatInspector) and the target sequences of zinc fingers: SPDEF1, SPDEF2, SPDEF3, and SPDEF4. Arrows show the orientation of the 18-bp binding site in the promoter. Location of ZF was shown relative to the TSS (+1). The translation start site is shown as ATG (+286). CpGs are indicated as vertical bars. DNA methylation status of 15 CpGs was analyzed using pyrosequencing for the indicated areas. Histone modification of H3K9me2 was assessed for the ChIP regions (gray boxs). *B*: relative *SPDEF* mRNA expression, normalized to the empty vector, was assessed by quantitative RT-PCR in transduced A549 cells. Data are presented as means and variation of three independent experiments. Statistical significance was analyzed using one-way ANOVA followed by Bonferroni's multiple-comparison test (*$P < 0.05$, **$P < 0.01$). *C*: SPDEF protein expression in transduced A549 cells, as conducted by Western blot analysis. An anti-GAPDH antibody was used as a loading control. An anti-FLAG antibody was used to detect the ATFs, which were designed with a C-terminal 3 × FLAG tag. Blot pictures shown are representative of two independent experiments.

Fisher Scientific) on an LightCycler 480 real-time PCR system (Roche). To calculate the fold induction/reduction of histone marks we used the formula: Percentage input = $2^{(\text{Cpinput}-\text{CpChIP})}$ dilution × factor × 100.

Detection of protein expression by Western blot analysis. Transduced A549 cells were lysed in RIPA buffer, and proteins were analyzed by standard Western blot analysis, as previously described (7). Then, the blots were incubated with a rabbit anti-human SPDEF antibody (sc-67022; Santa Cruz, Santa Cruz, CA), mouse anti-FLAG (F3165; Sigma) and mouse anti-GAPDH (sc-47724; Santa Cruz) at 4°C, overnight, followed by incubation with an horseradish peroxidase (HRP)-conjugated secondary goat anti-rabbit and rabbit anti-mouse antibody (Dako, Glostrup, Denmark). Protein expression was visualized using the Pierce ECL2 chemoluminescence detection kit (Thermo Fisher Scientific) and Gel Doc XR+ imaging systems (Bio-Rad Laboratories, Hercules, CA). Data were analyzed with Gel Doc XR+ Image Laboratory software.

Immunocytochemistry. Cells grown on coverslips (Menzel-Gläser, 12 mm in diameter) were washed with PBS and fixed with 2% (wt/vol) paraformaldehyde for 20 min. Cells were stained with primary antibody against MUC5AC (Abcam, ab3649), followed by HRP-conjugated secondary antibody. The peroxidase was visualized by staining with AEC (3-amino-9 ethylcarbazole), followed by hematoxylin counterstaining. The cover glasses were mounted with Kaiser's glycerol-gelatin (37°C) and scanned into digital whole slide images using the NanoZoomer series scanning devices. The assessment of immunochemistry staining intensity was performed semi-quantitatively in a blinded fashion at four to six of ×20 magnification fields. MUC5AC-stained cells were categorized as follows: negative (no staining), weak-positive (pink color or small red dot staining), and strong-positive (red staining and >50% of cell volume).

FLAG-tagged proteins were stained with anti-FLAG antibody (F3165; Sigma), followed by HRP-conjugated secondary antibody and AEC staining. FLAG-stained cells were categorized to negative and positive, and counted in a blinded fashion at four ×20 magnification fields.

Statistics. All transduction experiments were performed at least three times independently. Data were analyzed using one-way ANOVA followed by Bonferroni's multiple comparison test. Data were considered to be statistically significant if $P < 0.05$. Data were expressed as means ± SE and calculated using Prism v. 5.0 (GraphPad software).

RESULTS

SPDEF *downregulation by ATFs and subsequent repression of mucus-related genes.* To select a suitable model to study *SPDEF* downregulation, *SPDEF* expression was determined in four different human epithelial cell lines: A549, H292, BEAS-2B, and 16HBE. A549 cells demonstrated the highest expression of *SPDEF*, both at mRNA level (Fig. 1*A*) and at protein

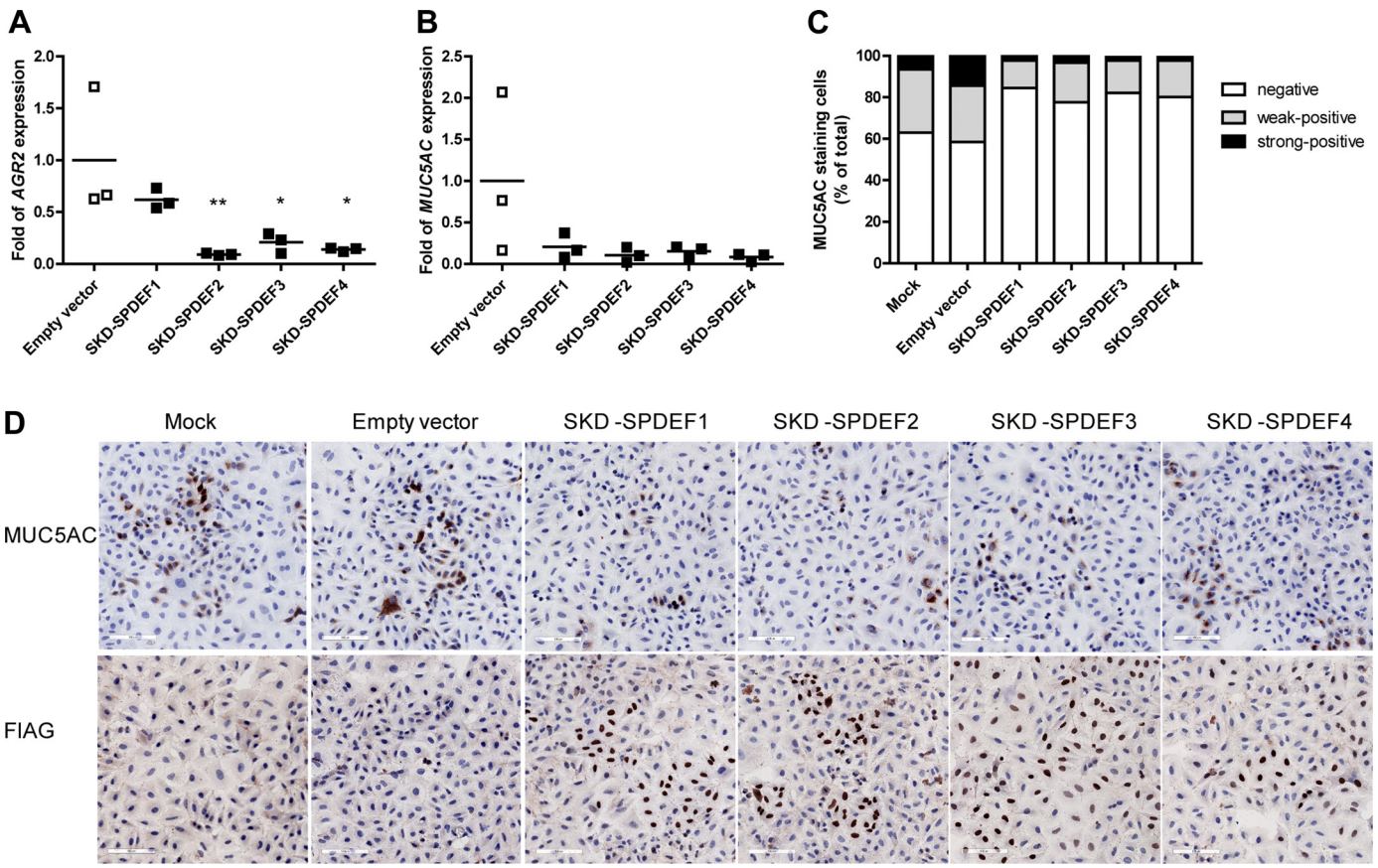

Fig. 3. Changes in downstream mucus-related genes after ATFs induced silencing of *SPDEF*. *MUC5AC* (*A*) and *AGR2* (*B*) mRNA expression were investigated by quantitative RT-PCR. Data are presented as means and variation of three independent experiments. Statistical significance was analyzed using one-way ANOVA followed by Bonferroni's multiple-comparison test (*$P < 0.05$, **$P < 0.01$). *C*: quantification of MUC5AC-negative, weak- and strong-positive A549 cells after ATF treatment. Counting of cells was performed in a blinded fashion. Solid bars, strong positive; shaded bars, weak positive; open bars, negative. Results represent the average of two independent experiments. *D*: representative photographs (original magnification, ×20) from immunochemistry staining for MUC5AC (*top*) and FLAG (*bottom*) in ATF-treated A549 cells. Red-stained cells are MUC5AC-positive and FLAG-positive, respectively. Nuclei were counterstained with hematoxylin. Scale bar: 100 μm.

level (Fig. 1*B*). The high expression of *SPDEF* in A549 and H292 cells was accompanied by a low degree of DNA methylation at the CpG sites surrounding the transcription start site (TSS) (A549: CpG sites no. 13: 2.7%, CpG sites no. 14: 4.6%, CpG sites no. 15: 3.1%; H292: CpG sites no. 13: 1.9%, CpG sites no. 14: 4.2%, CpG sites no. 15: 3.2%), whereas the undetectable transcription levels of *SPDEF* in BEAS-2B and 16HBE were accompanied by a high level of DNA methylation (BEAS-2B: CpG site no. 13, 34.9%; CpG site no. 14, 40.6%; CpG site no. 15, 26.4%; 16HBE: CpG sites no. 13, 75.9%; CpG sites no. 14, 68.5%; CpG sites no. 15, 41.0%) (Fig. 1*D*). Differential expression of *MUC5AC* was consistent with the observed *SPDEF* expression, with the highest *MUC5AC* expression in A549 cells (Fig. 1*C*). To explore effective *SPDEF* downregulation, we chose the highest *SPDEF* and *MUC5AC*-expressing cell line (A549) as a model.

To downregulate *SPDEF* expression, four ZFs were designed to bind 18-base pair regions in the *SPDEF* promoter (SPDEF1, SPDEF2, SPDEF3, and SPDEF4) and were subcloned into lentiviral constructs containing SKD (Fig. 2*A*). A549 cells were transduced to express the ATF using these lentiviral constructs. To enrich for cells expressing the ATF, the lentiviral transduced cells were positively selected on the basis of puromycin resistance. Correct size of ATFs was confirmed by Western blot analysis (Fig. 2*C*) and their nuclear location by immunohistochemical staining (Fig. 3*D*). FLAG-positive cells ranged from 15% (SKD-SPDEF2) to 64% (SKD-SPDEF3) after the selection with puromycin (Fig. 3*D*). According to the FLAG staining, SKD-SPDEF1 was expressed to a similar degree as SKD-SPDEF2, and both were generally expressed lower than SKD-SPDEF3 and SKD-SPDEF4.

Next, we examined the ability of the four ATFs to downregulate *SPDEF* mRNA expression in A549 cells. As shown in Fig. 2*B*, all four ATFs significantly downregulated *SPDEF* expression, demonstrating 70, 97, 93, and 96%, respectively, downregulation relative to empty vector control, which was confirmed at the protein level (Fig. 2*C*).

As *SPDEF* regulates a network of genes associated with mucus production (2, 20, 28), we investigated whether the downregulation of *SPDEF* expression mediated by ATFs, indeed, resulted in reduced expression of mucus-related genes. Therefore, the expression level of two downstream mucus-related genes was investigated in the ATF-expressing A549 cells. We found that expression of *AGR2* was significantly downregulated by SKD-SPDEF2 (90.9% ± 35.4% repression), SKD-SPDEF3 (79.3% ± 35.9% repression), and SKD-SPDEF4 (86.2% ± 35.4% repression) (Fig. 3*A*). *MUC5AC* was consistently, yet not significantly, downregulated in response to *SPDEF* repression (Fig. 3*B*). However, MUC5AC immunochemistry staining on ATF-transduced A549 cells supports successful inhibition at the protein level (Fig. 3, *C* and *D*).

SPDEF *silencing by targeted epigenetic editing.* To achieve the stable gene silencing, we set out to direct DNA methylation onto the *SPDEF* promoter. As DNA methylation levels of CpG sites no. 13 (−3 bp), no. 14 (−1 bp), and no. 15 (+40 bp) around the TSS negatively correlated with *SPDEF* expression,

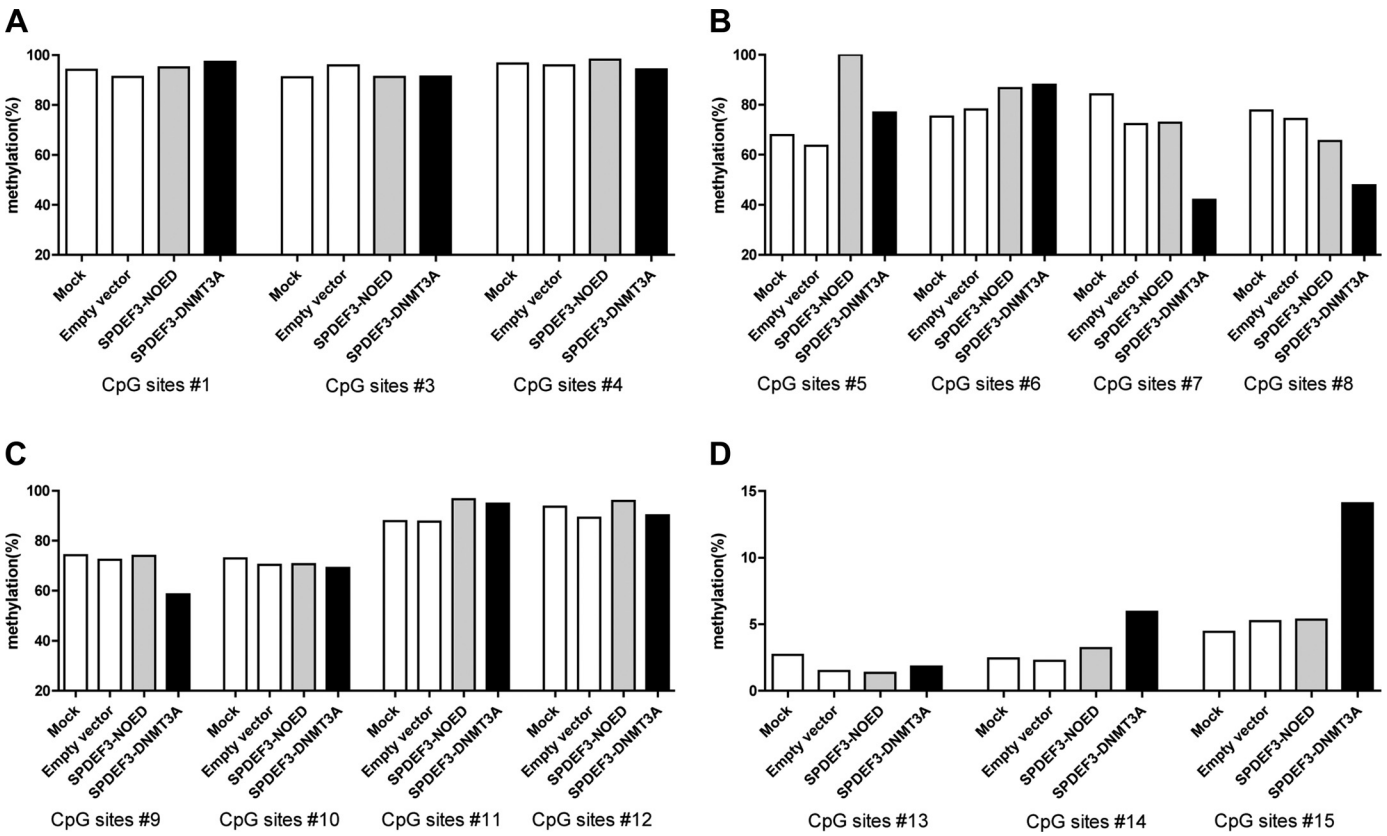

Fig. 4. Screening of the DNA methylation changes after targeting DNMT3A to *SPDEF* promoter. Quantitative analysis is the percentage of methylation for 14 CpG sites in *SPDEF* promoter by pyrosequencing in A549 cells treated with mock, empty vector, SPDEF3-NOED, and SPDEF3-DNMT3A in one experiment. *A*: CpG sites nos. 1, 3, and 4. *B*: CpG sites nos. 5–8. *C*: CpG sites nos.: 9–12. *D*: CpG sites nos. 13–15.

ZF SPDEF3 targeting location −131 to −114 bp was coupled to the catalytic domain of DNMT3A. To investigate the induced DNA methylation in the promoter region of *SPDEF*, 15 CpG sites were screened with pyrosequencing (Fig. 4). We found that DNA methylation was induced on CpG sites nos. 14 and 15, but not on CpG sites nos. 1–13. In further experiments, CpG sites nos. 13–15 were analyzed. SPDEF3-DNMT3A consistently deposited DNA methylation onto two CpG sites (CpG no. 14: 6.6 ± 0.8%; CpG no. 15: 10.5 ± 1.3%), compared with SPDEF3-NOED (CpG no. site 14: 3.9 ± 0.3%; CpG no. 15: 5.2 ± 0.8%) (Fig. 5*B*). To determine whether the observed increase in DNA methylation was directly caused by the catalytic activity of the DNMT3A enzyme, a catalytic mutant of DNMT3A (DNMT3A E74A) was constructed and compared with DNMT3A in a separate set of experiments. No increase in DNA methylation was observed for CpG sites no. 13–15 in SPDEF3-DNMT3A E74A-treated cells (Fig. 5*C*). To investigate whether the ZF-directed DNMT3A was able to reduce target gene transcription, *SPDEF* mRNA expression was investigated (Fig. 6*A*, *left*). SPDEF3-DNMT3A was able to downregulate *SPDEF* expression (76.6% ± 25.5% repression), which was equally efficient as repression induced by the positive control SKD-SPDEF3 (79.1% ± 12.7% repression). Interestingly, the construct that lacked the effector domain, SPDEF3-NOED, also reduced *SPDEF* expression significantly (72.0% ± 25.3% repression). To determine the influence of location, another ZF (SPDEF4: target sequence +112 to +129) was tested to target DNMT3A to the *SPDEF* promoter. We found that SPDEF4-DNMT3A was able to better downregulate *SPDEF* expression (86.9% ± 12.1% repression) than control SPDEF4-NOED (46.8% ± 35.1% *SPDEF* repression) and the catalytic mutant (Fig. 6*A*), even though SPDEF4-DNMT3A did not induce methylation changes in the investigated region CpG13–15 (Fig. 5*D*).

Upon ZFs fusion with the histone methyltransferase G9A, again, SPDEF4-G9A was able to downregulate *SPDEF* expression equally efficiently as positive control SKD-SPDEF4 and further repressed *SPDEF* expression than SPDEF4-NOED (Fig. 6*A*). However, no difference was detected between SPDEF4-G9A and its mutant, and no H3K9me2 marks were detected in the examined region (data not shown). The expression of the fusion proteins was confirmed by the mRNA expression of the FLAG-tag (Fig. 7). The SPDEF4-DNMT3A construct was not higher expressed than its mutant, indicating that enhanced

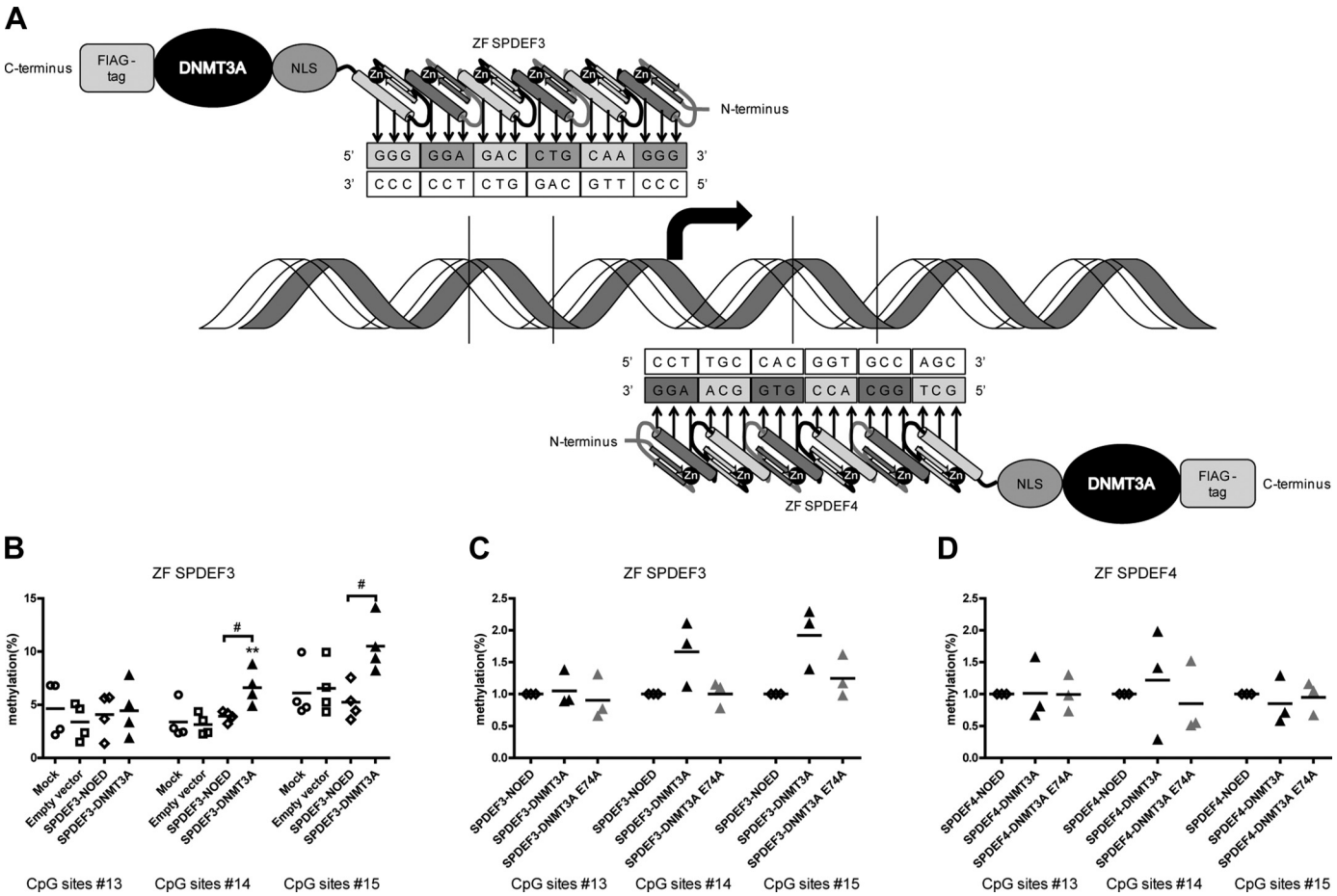

Fig. 5. DNA methylation changes after targeting DNMT3A to *SPDEF* promoter. *A*: schematic presentation of SPDEF3-DNMT3A and SPDEF4-DNMT3A, and their binding location relative to TSS. *B*: quantitative analysis of the methylation percentage for target CpG sites (nos. 13, 14 and 15) by pyrosequencing in A549 cells treated with mock, empty vector, SPDEF3-NOED and SPDEF3-DNMT3A ($n = 4$). *C*: relative DNA methylation level of A549 cells after treatment with SPDEF3-NOED, SPDEF3-DNMT3A, and SPDEF3-DNMT3A E74A normalized to SPDEF3-NOED ($n = 3$). *D*: relative DNA methylation level of A549 cells after treatment with SPDEF4-NOED, SPDEF4-DNMT3A, and SPDEF4-DNMT3A E74A normalized to SPDEF4-NOED ($n = 3$). Dot plots represent the mean and variation of at least three independent experiments. Statistical significance was analyzed using one-way ANOVA followed by Bonferroni's multiple-comparison test (**$P < 0.01$, compared with empty vector; #$P < 0.05$, compared between two indicated columns).

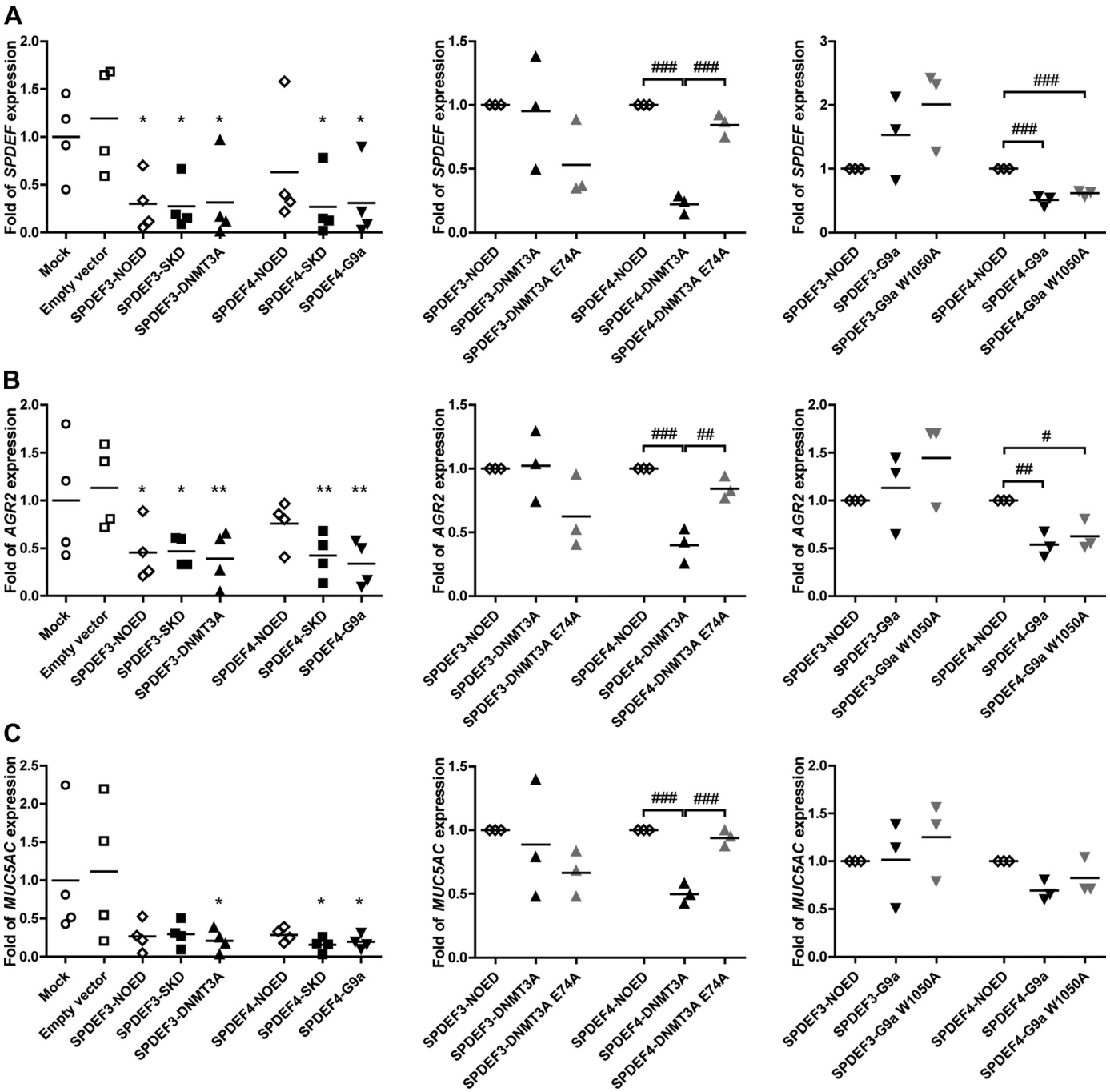

Fig. 6. *SPDEF* and downstream mucus-related genes expression changes after targeting DNMT3A and G9a to *SPDEF* promoter. A549 cells were treated with ZFs fused with different effector domains (SKD, DNMT3A, G9a, and the respective mutants DNMT3A, E74A, and G9a W1050A). mRNA level of *SPDEF* (*A*), *AGR2* (*B*), and *MUC5AC* (*C*) were determined by quantitative RT-PCR on treated A549 cells. The expression of *SPDEF* was relative to *GAPDH* and normalized to mock-treated cells (*left*), or normalized to ZF-NOED (*middle* and *right*) to enlarge any difference between wild-type and mutant effectors. Dot plots represent the mean and variation of at least three independent experiments. Statistical significance was analyzed using one-way ANOVA followed by Bonferroni's multiple-comparison test (*$P < 0.05$, **$P < 0.01$, compared with empty vector; ##$P < 0.01$, ###$P < 0.001$, compared between two indicated columns).

SPDEF repression of SPDEF4-DNMT3A compared with its mutant was not because of more occupation of ZFs SPDEF4 itself.

Downregulation of *SPDEF* by SPDEF3-DNMT3A, SPDEF4-DNMT3A, SPDEF3-G9A, and SPDEF4-G9A was confirmed at the protein level by Western blot analysis (Fig. 8). Importantly, the expression of downstream mucus-related genes *AGR2* and *MUC5AC* was also downregulated by these constructs (Fig. 6, *B* and *C*).

Lower number of strong MUC5AC positive cells after targeted silencing SPDEF *by epigenetic editing.* The effect of *SPDEF* inhibition on mucus production was determined by quantification of the number of MUC5AC-positive cells. Transduced A549 cells were seeded on coverslips and exam-

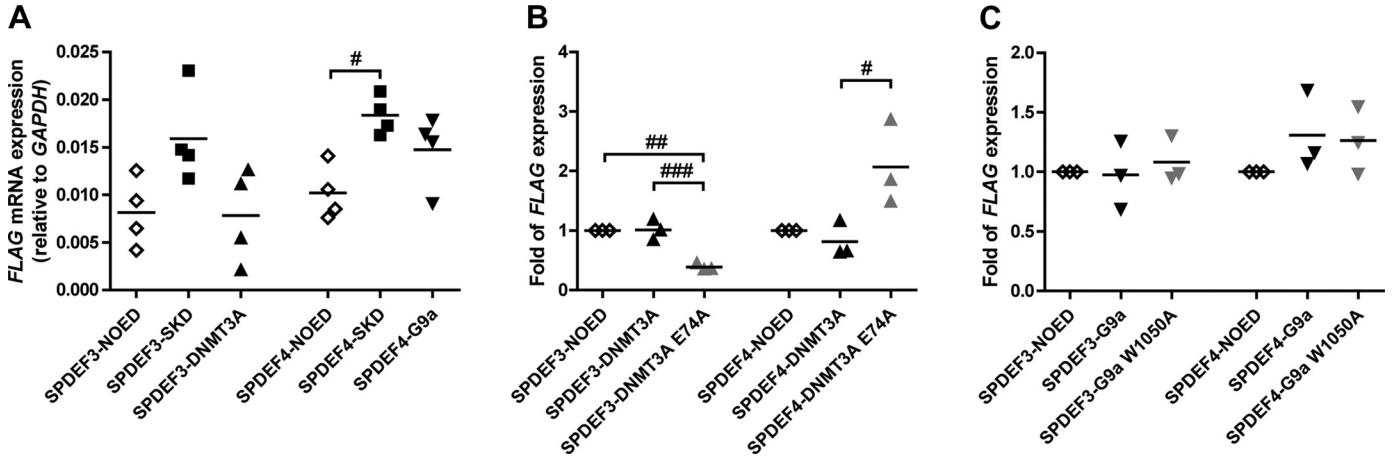

Fig. 7. Expression of ZF-ED after A549 cells treated with ZF fused to different effector domain (SKD, DNMT3A, G9a, and respective mutant DNMT3A E74A and G9a W1050A). The expression of ZF-ED was represented as the FLAG-tag expression relative to *GAPDH* (*A*), and normalized to ZF-NOED (*B* and *C*). Dot plots represent the mean and variation of three independent experiments. Statistical significance was analyzed using one-way ANOVA followed by Bonferroni's multiple-comparison test (#$P < 0.05$, ##$P < 0.01$, ###$P < 0.001$, compared between two indicated columns).

ined by immunochemistry staining. Interestingly, *SPDEF* silencing was most effective within the MUC5AC strong-positive cell population. Within this population, both SPDEF3-DNMT3A and SPDEF4-G9a treatment resulted in lower numbers of MUC5AC strong-positive (Fig. 9*B*). To rule out that the effects were caused by a general repressive effect of either G9A or DNMT3A, we determined expression levels of four irrelevant genes (*PLOD2*, *TP53*, *RELA*, and *CDKN1A*) and found that none of these demonstrated inhibition of expression (Fig. 10).

Sustained epigenetic repression of SPDEF *by epigenetic editing.* To further address the effectiveness and sustainability of gene repression by epigenetic editing, we decided to use the CRISPR-dCas9 system. We engineered stable MCF7 cell lines, each one expressing dCas9 fusions either with the transcriptional repressor SKD, several epigenetic editors or their mutants G9a and SUV39h1 (for H3K9me), the SET domain of EZH2 (for H3K27me), or a chimeric DNMT3a-DNMT3L fusion [for DNA methylation (30)]. We designed three gRNAs to bind around the promoter of SPDEF. By transiently transfecting a mix of the three gRNAs into the stable cell lines, we were able to address the maintenance of gene repression (Fig. 11*A*). Gene repression was achieved to similar degrees 2 days after transfecting the mix of gRNAs in all stable cell lines. As observed for ZF fusions, repression was also observed when using the mutant effector domains (Fig. 11, *B–E*). Importantly, for several other genes, no such repressive effects by dCas9 without effector domain have been observed in this stable system (data not shown). While repression by the transcriptional repressor SKD and most of the epigenetic editors was not maintained, the repression of SPDEF was sustained when using the G9a effector domain, while the mutant fusion regained activation.

DISCUSSION

On the basis of its important role in goblet cell differentiation and mucus production (6, 26), we reasoned that *SPDEF* could be a suitable therapeutic target against mucus hypersecretion. In this study, we were able to silence *SPDEF* expression in the human alveolar epithelial cell line A549, using a novel strategy: engineered *SPDEF* targeting ZF proteins directing transcriptional repressor (SKD), as well as epigenetic enzymes (DNMT3A and G9A). The repression of *SPDEF* was accompanied by lower expression of mucus-related genes *MUC5AC* and *AGR2*, as well as lower numbers of MUC5AC-positive cells.

Our data provide an original proof-of-concept study supporting *SPDEF* as a promising therapeutic target for inhibiting mucus production, which is amenable to stable repression with epigenetic editing. As previously reported, knockdown of *SPDEF* using siRNA was able to reduce the IL-13-induced expression of MUC5AC and AGR2 in human airway epithelial 16HBE cells (36). The principle of siRNA is to target and degrade mRNA. Because of the constant production of mRNA, the silencing effect of siRNA is generally transient, and it has to be delivered repeatedly in clinical application. Epigenetic editing would be a superior strategy because the effect would be sustained after clearance of the drug (hit and run approach) (8). To downregulate SPDEF expression directly at the transcriptional level, four sequence-specific ZFs were generated. ZFs were first linked to SKD to test the functionality of the DNA binding domain because SKD can cause transient gene silencing by indirectly recruiting chromatin remodelers and histone-modifying enzymes (28, 32). These four ATFs (ZF-SKD) strongly reduced *SPDEF* expression and nearly abolished all expression of *SPDEF* in A549 cells. More importantly, *SPDEF* silencing resulted in the additional downregulation of MUC5AC mRNA and protein expression as well, indicating successful inhibition of mucin synthesis.

Next, ZFs were fused to catalytic domains of epigenetic enzymes (DNMT3A and G9A), aiming for longer-term gene silencing by changing the epigenetic state of the targeted gene. ZF-targeted DNA methylation was recently successfully used for silencing several cancer-associated genes, including VEGF-A, SOXA2, and EpCAM (24, 28, 29, 31). Here, we took advantage of this approach by using two different ZFs engineered close to the TSS (SPDEF3 and SPDEF4), to downregulate *SPDEF* expression. In this area, high expression of *SPDEF* was accompanied by lower DNA methylation of CpG sites, particularly those surrounding the TSS, where DNA

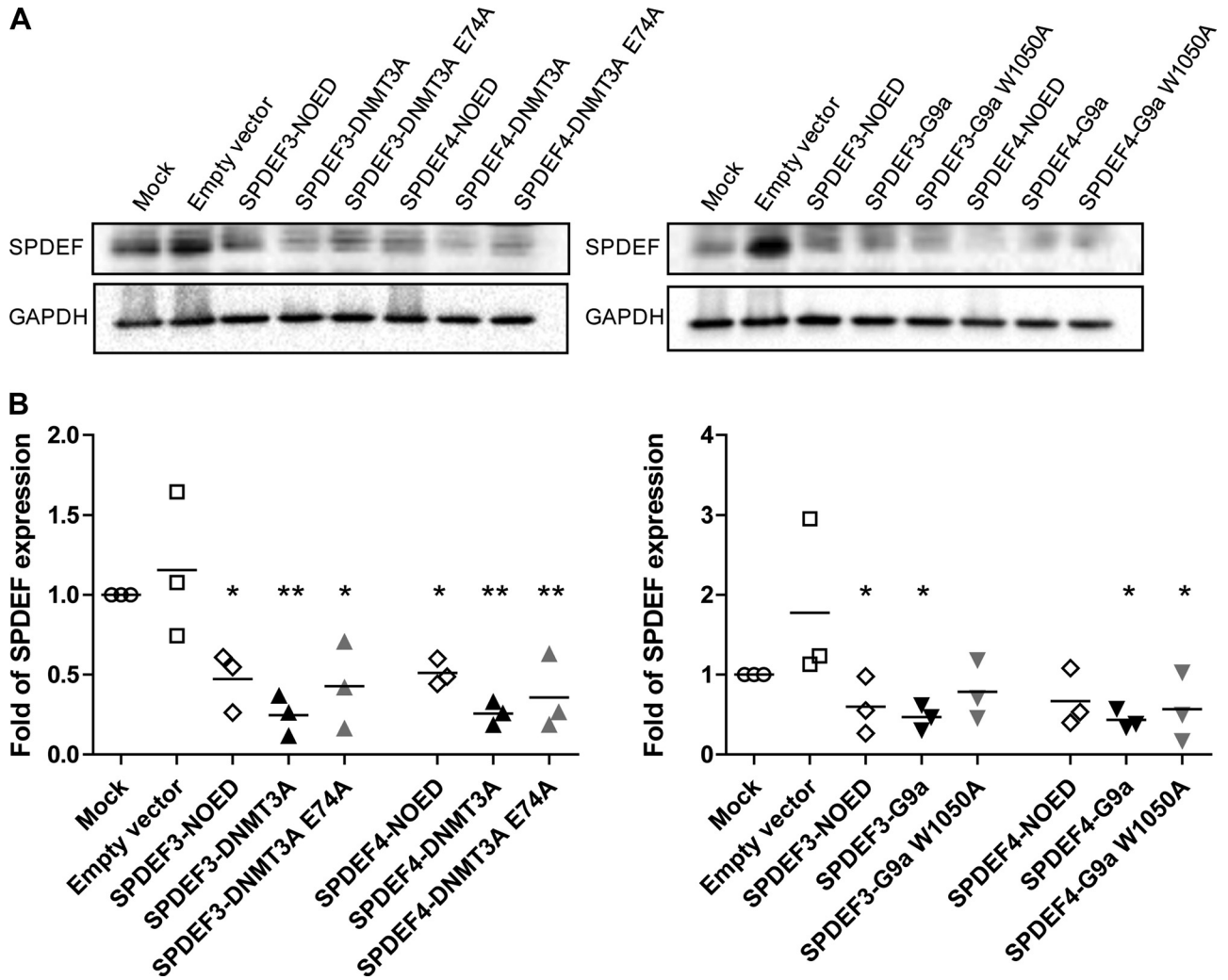

Fig. 8. Quantification of the changes of SPDEF protein levels in A549 cells treated with *SPDEF*-targeted DNMT3A and G9a. A549 cells were treated with ZF fused with different effector domains (SKD, DNMT3A, G9a, and respective mutant DNMT3A E74A and G9a W1050A). *A*: protein expression of SPDEF was assessed by Western blot analysis. An anti-GAPDH antibody was used as a loading control. Blot pictures shown are representative of three independent experiments. *B*: densitometric values of SPDEF were normalized against the loading control, GAPDH. The relative level (ratio to mock) of SPDEF was shown with the average of three independent experiments. Statistical significance was analyzed using one-way ANOVA followed by Bonferroni's multiple comparison test (*$P < 0.05$, **$P < 0.01$, compared with empty vector).

methylation is tightly linked to transcriptional silencing (3). The occlusion binding of TF also explains our observation that ZFs without effector domains effectively silenced *SPDEF* expression. We observed similar strong SPDEF-repressive effects upon targeting ZFs without any effector domain as upon targeting ZFs fused with repressor SKDs. Many factors can explain the repressive effects of the binding of the gene-targeting constructs, like competition with endogenous transcription factors, such as SMAD, or components of the preinitiation complex formation. Importantly, the effects were also obtained when targeting CRISPR-dCas9 without an effector by the sgRNAs (20), indicating that steric hindrance might, indeed, explain the repressive effect. Because such effects generally are transient, it is important to assess that the addition of domains to the targeting moiety do not affect inhibition properties. Importantly, the fusion of effector domains to the ZFs did not hamper the repressive effect of the ZF approach.

As the DNA binding domain by itself, or in fusion with SKD, is not expected to induce any long-term effects, we next set out to test different epigenetic enzymes (DNMT3A and G9A). Fusion of epigenetic effector domains with ZFs resulted in the same magnitude of silencing as the ZF-SKD fusions, indicating that our approach worked as we aimed. Furthermore, targeted DNA methylation or histone methylation has the advantage that its effect has the potential to be permanent (4, 28, 31), albeit the stability and heritability of epigenetic editing are still controversial (14, 19) and likely depend on the local chromatin modification state (4).

In an elegant experiment, Bintu et al. (2)used an artificial system to compare four repressive chromatin regulators with distinct chromatin modifications: the embryonic ectoderm development protein of Polycomb-repressive complex 2, which indirectly catalyzes H3K27 methylation; the KRAB domain, which indirectly promotes H3K9 methylation; the DNMT3B, which catalyzes DNA methylation; and the histone deacetylase 4 (HDAC4) enzyme. By transiently recruiting each protein, they demonstrate that different types of repressed chromatin are generally associated with distinct time scales of repression.

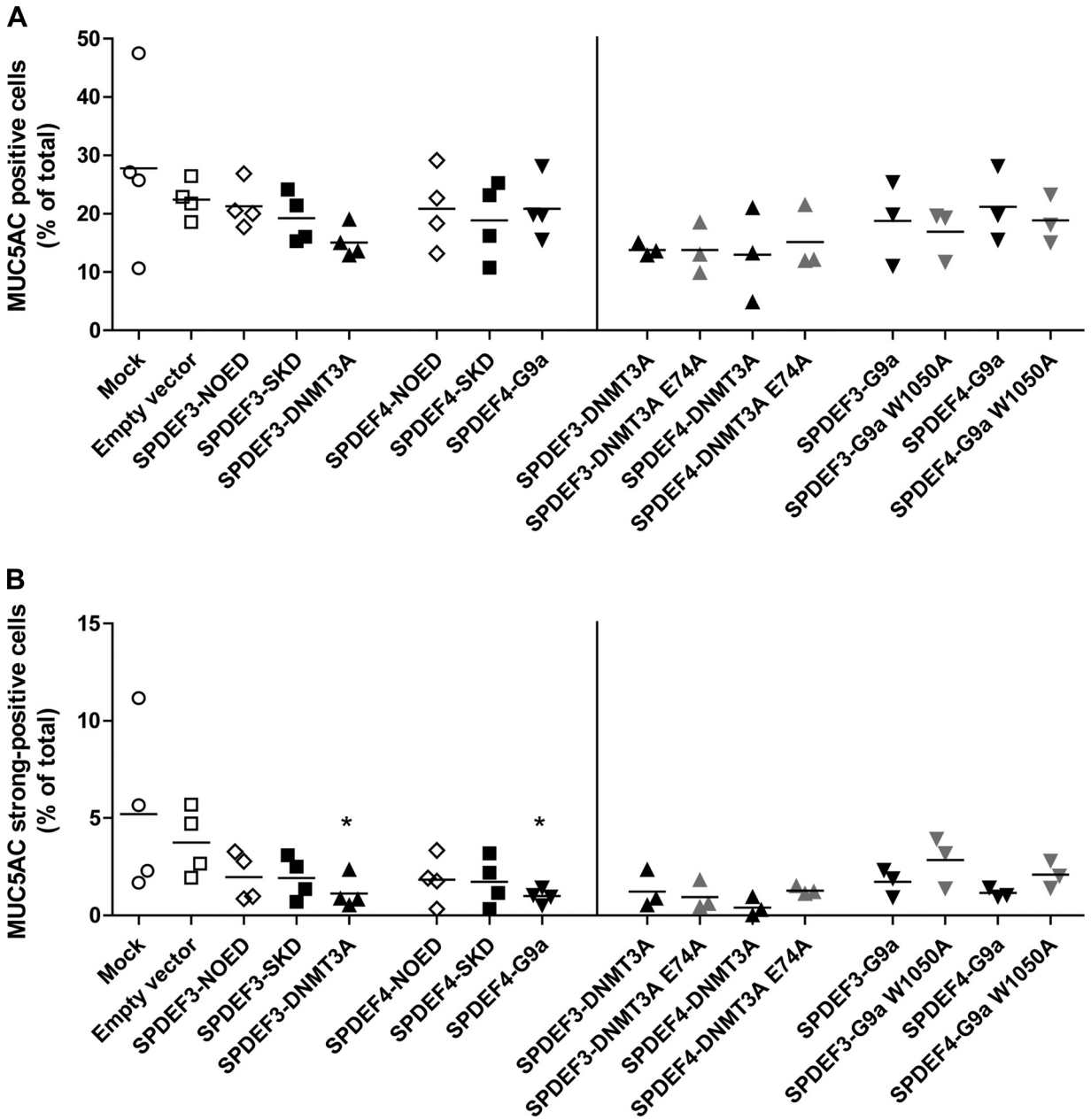

Fig. 9. Quantification of MUC5AC-positive A549 cells after treatment with *SPDEF* targeted DNMT3A and G9a. A549 cells were treated with ZFs fused with different effector domains (SKD, DNMT3A, G9a, and respective mutant DNMT3A E74A and G9a W1050A) and grown on coverslips. Immunochemistry staining for MUC5AC was quantified to negative, weak-positive, and strong-positive in a blinded fashion. *A*: percentage of MUC5AC-positive cells in the total cell populations. *B*: percentage of MUC5AC strong-positive cells in the total cell populations. Results are represented as mean and variation of three independent experiments. Statistical significance was analyzed using one-way ANOVA followed by Bonferroni's multiple-comparison test (*$P < 0.05$, compared with empty vector).

For this artificial context, DNA methylation was the modification of choice to achieve long-lasting repression, while histone deacetylation was not sustained. Only a few studies so far have addressed stable silencing of endogenous genes, and controversial effects have been reported (1, 19, 31). Here, we provide indications that targeting epigenetic effector domains to *SPDEF* has the ability to promote sustained gene expression reprogramming. Indeed, we demonstrated that upon targeting G9A, maintenance of repression was obtained, which was not observed for the transcriptional repressor SKD, DNA methyltransferase, or other histone modifiers. These differences in maintenance require more thorough investigations, but likely, they are due to the particular local chromatin context of the targeted locus, which could influence the potency and longevity of epigenetic reprogramming. This would also explain the reported failure of maintenance of induced H3K9 methylation effects when studying VEGF-A repression (19). Combining different effector domains, as we did previously for reactivation of gene expression, might further improve the degree of repression and/or increase sustainability (4). Indeed, Amabile et al. (1) recently demonstrated the importance of cotargeting KRAB,

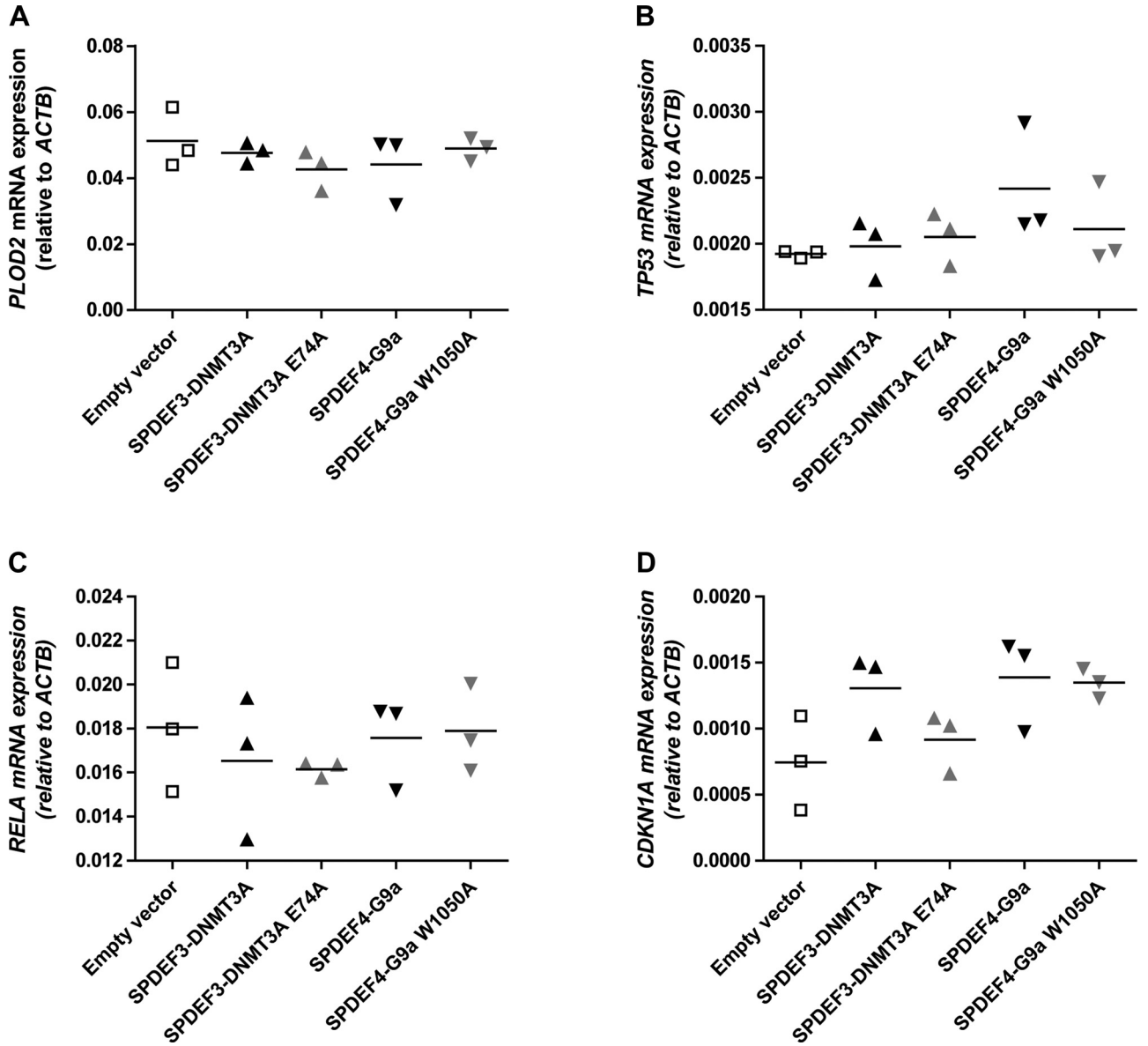

Fig. 10. Expression of irrelevant genes after A549 cells treated with ZF fused to different effector domain (DNMT3A, G9a, and respective mutant DNMT3A E74A and G9a W1050A). The expression of *PLOD2* (*A*), *TP53* (*B*), *RELA* (*C*), and *CDKN1A* (*D*) was relative to *ACTB*. The dot plots represent the mean and variation of three independent experiments.

DNMT3A, and DNMT3L in inducing maintained repression for endogenous genes.

One limitation of our study is that functional experiments were conducted in the alveolar cell line A549. Because we already showed convincing evidence of *MUC5AC* and *AGR2* silencing in A549 cells, it will be interesting to investigate whether this effect is also observed within the more relevant models of mucus hypersecretion in the future, such as using the air-liquid interface culture of the primary airway epithelial cells from patients with COPD. In addition, before use in the clinical setting, it is necessary to further evaluate the off-target effects, such as the ZFs or CRISPR/dCas9 binding specificity and target cell specificity.

In summary, we successfully reduced mucus-related gene expression by targeted silencing of *SPDEF*. This new approach (epigenetic editing) has the potential to induce a permanent anti-mucus effect, which has implications for development of novel therapeutic strategies to treat patients with chronic mucus hypersecretion in the future.

ACKNOWLEDGMENTS

The authors would like to thank J. M. Dokter-Fokkens, P. G. Jellema, M. G. P. van der Wijst, and K. Meyer, Department of Pathology and Medical Biology, University Medical Center Groningen, for technical help with this study.

GRANTS

This work was supported by grants from the Stichting Astma Bestrijding (project 2014/007) and the Jan Kornelis de Cock Stichting (project 2014–62). J. Song is supported by the Abel Tasman Talent Program, University Medical Center Groningen. D. Cano-Rodriguez is supported by Samenwerkingsverband Noord-Nederland SNN-4D22C-T2007. D. Goubert is supported by European Union funding H2020-MSCA-ITN-2014-ETN 642691 EpiPredict. T. P.

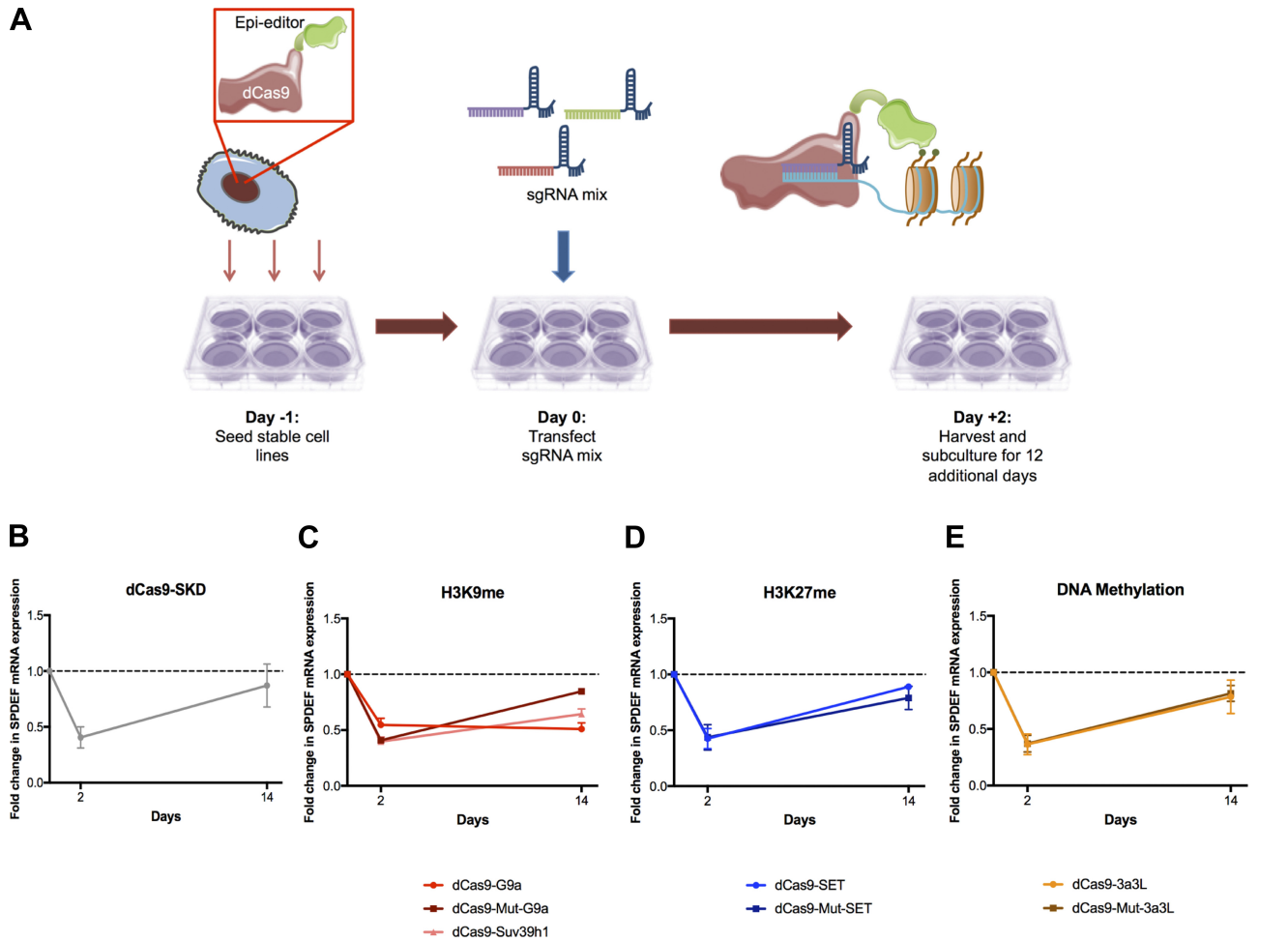

Fig. 11. Sustained gene repression by means of epigenetic editing using the CRISPR-dCas9 system. *A*: schematic representation of the experimental setup with the stable MCF7 cells. mRNA level of *SPDEF* determined by quantitative RT-PCR on MCF7 stable cells with dCas9-SKD (*B*), G9a, its mutant, and Suv39h1 (*C*) SET and its mutant (*D*) and DNMT3a3L and its mutant (*E*). Results are represented as average ± SE of three independent experiments.

Jurkowski is supported by Baden-Württemberg Stiftung (95011370). M. Hylkema is Management Committee member of Cooperation in Science and Technology (COST) Action BM1201. M. G. Rots is vice-chair of COST Action CM 1406 (EpiChemBio.eu).

DISCLOSURES

No conflicts of interest, financial or otherwise, are declared by the authors.

AUTHOR CONTRIBUTIONS

J.S., D.C.R., M.W., R.A.G., T.P.J., I.H.H., M.G.R., and M.N.H. conceived and designed research; J.S., D.C.R., M.W., D.G., and T.P.J. performed experiments; J.S., D.C.R., D.G., and M.N.H. analyzed data; J.S., D.C.R., D.G., M.G.R., and M.N.H. interpreted results of experiments; J.S., D.C.R., M.G.R., and M.N.H. prepared figures; J.S., D.C.R., M.G.R., and M.N.H. drafted manuscript; J.S., D.C.R., M.W., R.A.G., D.G., T.P.J., I.H.H., M.G.R., and M.N.H. edited and revised manuscript; J.S., D.C.R., M.W., R.A.G., D.G., T.P.J., I.H.H., M.G.R., and M.N.H. approved final version of manuscript.

REFERENCES

1. **Amabile A, Migliara A, Capasso P, Biffi M, Cittaro D, Naldini L, Lombardo A.** Inheritable silencing of endogenous genes by hit-and-run targeted epigenetic editing. *Cell* 167: 219.e14–232.e14, 2016. doi:10.1016/j.cell.2016.09.006.
2. **Bintu L, Yong J, Antebi YE, McCue K, Kazuki Y, Uno N, Oshimura M, Elowitz MB.** Dynamics of epigenetic regulation at the single-cell level. *Science* 351: 720–724, 2016. doi:10.1126/science.aab2956.
3. **Brenet F, Moh M, Funk P, Feierstein E, Viale AJ, Socci ND, Scandura JM.** DNA methylation of the first exon is tightly linked to transcriptional silencing. *PLoS One* 6: e14524, 2011. doi:10.1371/journal.pone.0014524.
4. **Cano-Rodriguez D, Gjaltema RA, Jilderda LJ, Jellema P, Dokter-Fokkens J, Ruiters MH, Rots MG.** Writing of H3K4Me3 overcomes epigenetic silencing in a sustained but context-dependent manner. *Nat Commun* 7: 12284, 2016. doi:10.1038/ncomms12284.
5. **Cano-Rodriguez D, Rots MG.** Epigenetic editing: on the verge of reprogramming gene expression at will. *Curr Genet Med Rep* 4: 170–179, 2016. doi:10.1007/s40142-016-0104-3.
6. **Chen G, Korfhagen TR, Xu Y, Kitzmiller J, Wert SE, Maeda Y, Gregorieff A, Clevers H, Whitsett JA.** SPDEF is required for mouse pulmonary goblet cell differentiation and regulates a network of genes associated with mucus production. *J Clin Invest* 119: 2914–2924, 2009. doi:10.1172/JCI39731.
7. **Chen H, Kazemier HG, de Groote ML, Ruiters MH, Xu GL, Rots MG.** Induced DNA demethylation by targeting Ten-Eleven Translocation 2 to the human *ICAM*-1 promoter. *Nucleic Acids Res* 42: 1563–1574, 2014. doi:10.1093/nar/gkt1019.
8. **de Groote ML, Verschure PJ, Rots MG.** Epigenetic editing: targeted rewriting of epigenetic marks to modulate expression of selected target genes. *Nucleic Acids Res* 40: 10596–10613, 2012. doi:10.1093/nar/gks863.
9. **Fahy JV, Dickey BF.** Airway mucus function and dysfunction. *N Engl J Med* 363: 2233–2247, 2010. doi:10.1056/NEJMra0910061.
10. **Falahi F, Huisman C, Kazemier HG, van der Vlies P, Kok K, Hospers GA, Rots MG.** Towards sustained silencing of HER2/neu in cancer by

epigenetic editing. *Mol Cancer Res* 11: 1029–1039, 2013. doi:10.1158/1541-7786.MCR-12-0567.

11. **Gao W, Li L, Wang Y, Zhang S, Adcock IM, Barnes PJ, Huang M, Yao X.** Bronchial epithelial cells: the key effector cells in the pathogenesis of chronic obstructive pulmonary disease? *Respirology* 20: 722–729, 2015. doi:10.1111/resp.12542.
12. **Gjaltema RAF, de Rond S, Rots MG, Bank RA.** Procollagen lysyl hydroxylase 2 expression is regulated by an alternative downstream transforming growth factor β-1 activation mechanism. *J Biol Chem* 290: 28,465–28,476, 2015. doi:10.1074/jbc.M114.634311.
13. **Gowher H, Loutchanwoot P, Vorobjeva O, Handa V, Jurkowska RZ, Jurkowski TP, Jeltsch A.** Mutational analysis of the catalytic domain of the murine Dnmt3a DNA-(cytosine C5)-methyltransferase. *J Mol Biol* 357: 928–941, 2006. doi:10.1016/j.jmb.2006.01.035.
14. **Hathaway NA, Bell O, Hodges C, Miller EL, Neel DS, Crabtree GR.** Dynamics and memory of heterochromatin in living cells. *Cell* 149: 1447–1460, 2012. doi:10.1016/j.cell.2012.03.052.
15. **Heijink IH, Brandenburg SM, Noordhoek JA, Postma DS, Slebos D-J, van Oosterhout AJM.** Characterisation of cell adhesion in airway epithelial cell types using electric cell-substrate impedance sensing. *Eur Respir J* 35: 894–903, 2010. doi:10.1183/09031936.00065809.
16. **Huisman C, Wisman GB, Kazemier HG, van Vugt MA, van der Zee AG, Schuuring E, Rots MG.** Functional validation of putative tumor suppressor gene C13ORF18 in cervical cancer by artificial transcription factors. *Mol Oncol* 7: 669–679, 2013. doi:10.1016/j.molonc.2013.02.017.
17. **Jurkowski TP, Ravichandran M, Stepper P.** Synthetic epigenetics-towards intelligent control of epigenetic states and cell identity. *Clin Epigenetics* 7: 18, 2015. doi:10.1186/s13148-015-0044-x.
18. **Kearns NA, Genga RM, Enuameh MS, Garber M, Wolfe SA, Maehr R.** Cas9 effector-mediated regulation of transcription and differentiation in human pluripotent stem cells. *Development* 141: 219–223, 2014. doi:10.1242/dev.103341.
19. **Kungulovski G, Nunna S, Thomas M, Zanger UM, Reinhardt R, Jeltsch A.** Targeted epigenome editing of an endogenous locus with chromatin modifiers is not stably maintained. *Epigenetics Chromatin* 8: 12, 2015. doi:10.1186/s13072-015-0002-z.
20. **Larson MH, Gilbert LA, Wang X, Lim WA, Weissman JS, Qi LS.** CRISPR interference (CRISPRi) for sequence-specific control of gene expression. *Nat Protoc* 8: 2180–2196, 2013. doi:10.1038/nprot.2013.132.
21. **Martin C, Frija-Masson J, Burgel PR.** Targeting mucus hypersecretion: new therapeutic opportunities for COPD? *Drugs* 74: 1073–1089, 2014. doi:10.1007/s40265-014-0235-3.
22. **McCauley HA, Guasch G.** Three cheers for the goblet cell: maintaining homeostasis in mucosal epithelia. *Trends Mol Med* 21: 492–503, 2015. doi:10.1016/j.molmed.2015.06.003.
23. **Miravitlles M.** Cough and sputum production as risk factors for poor outcomes in patients with COPD. *Respir Med* 105: 1118–1128, 2011. doi:10.1016/j.rmed.2011.02.003.
24. **Nunna S, Reinhardt R, Ragozin S, Jeltsch A.** Targeted methylation of the epithelial cell adhesion molecule (EpCAM) promoter to silence its expression in ovarian cancer cells. *PLoS One* 9: e87703, 2014. doi:10.1371/journal.pone.0087703.
25. **Park KS, Korfhagen TR, Bruno MD, Kitzmiller JA, Wan H, Wert SE, Khurana Hershey GK, Chen G, Whitsett JA.** SPDEF regulates goblet cell hyperplasia in the airway epithelium. *J Clin Invest* 117: 978–988, 2007. doi:10.1172/JCI29176.
26. **Rajavelu P, Chen G, Xu Y, Kitzmiller JA, Korfhagen TR, Whitsett JA.** Airway epithelial SPDEF integrates goblet cell differentiation and pulmonary Th2 inflammation. *J Clin Invest* 125: 2021–2031, 2015. doi:10.1172/JCI79422.
27. **Ramos FL, Krahnke JS, Kim V.** Clinical issues of mucus accumulation in COPD. *Int J Chron Obstruct Pulmon Dis* 9: 139–150, 2014. doi:10.2147/COPD.S38938.
28. **Rivenbark AG, Stolzenburg S, Beltran AS, Yuan X, Rots MG, Strahl BD, Blancafort P.** Epigenetic reprogramming of cancer cells via targeted DNA methylation. *Epigenetics* 7: 350–360, 2012. doi:10.4161/epi.19507.
29. **Siddique AN, Nunna S, Rajavelu A, Zhang Y, Jurkowska RZ, Reinhardt R, Rots MG, Ragozin S, Jurkowski TP, Jeltsch A.** Targeted methylation and gene silencing of VEGF-A in human cells by using a designed Dnmt3a-Dnmt3L single-chain fusion protein with increased DNA methylation activity. *J Mol Biol* 425: 479–491, 2013. doi:10.1016/j.jmb.2012.11.038.
30. **Stepper P, Kungulovski G, Jurkowska RZ, Chandra T, Krueger F, Reinhardt R, Reik W, Jeltsch A, Jurkowski TP.** Efficient targeted DNA methylation with chimeric dCas9-Dnmt3a-Dnmt3L methyltransferase. *Nucleic Acids Res* gkw1112, 2016. 10.1093/nar/gkw1112.
31. **Stolzenburg S, Beltran AS, Swift-Scanlan T, Rivenbark AG, Rashwan R, Blancafort P.** Stable oncogenic silencing in vivo by programmable and targeted de novo DNA methylation in breast cancer. *Oncogene* 34: 5427–5435, 2015. doi:10.1038/onc.2014.470.
32. **Stolzenburg S, Rots MG, Beltran AS, Rivenbark AG, Yuan X, Qian H, Strahl BD, Blancafort P.** Targeted silencing of the oncogenic transcription factor SOX2 in breast cancer. *Nucleic Acids Res* 40: 6725–6740, 2012. doi:10.1093/nar/gks360.
33. **Thakore PI, Black JB, Hilton IB, Gersbach CA.** Editing the epigenome: technologies for programmable transcription and epigenetic modulation. *Nat Methods* 13: 127–137, 2016. doi:10.1038/nmeth.3733.
34. **Thomson NC, Chaudhuri R, Messow CM, Spears M, MacNee W, Connell M, Murchison JT, Sproule M, McSharry C.** Chronic cough and sputum production are associated with worse clinical outcomes in stable asthma. *Respir Med* 107: 1501–1508, 2013. doi:10.1016/j.rmed.2013.07.017.
35. **Wang G, Xu Z, Wang R, Al-Hijji M, Salit J, Strulovici-Barel Y, Tilley AE, Mezey JG, Crystal RG.** Genes associated with MUC5AC expression in small airway epithelium of human smokers and non-smokers. *BMC Med Genomics* 5: 21, 2012. doi:10.1186/1755-8794-5-21.
36. **Yu H, Li Q, Kolosov VP, Perelman JM, Zhou X.** Interleukin-13 induces mucin 5AC production involving STAT6/SPDEF in human airway epithelial cells. *Cell Commun Adhes* 17: 83–92, 2010. doi:10.3109/15419061.2010.551682.